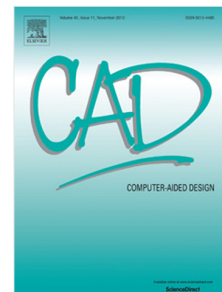


# Accepted Manuscript

Range image registration based on 2D synthetic images

Sukwoo Jung, Seunghyun Song, Minho Chang, Sangchul Park



PII: S0010-4485(17)30135-5

DOI: <http://dx.doi.org/10.1016/j.cad.2017.08.001>

Reference: JCAD 2543

To appear in: *Computer-Aided Design*

Received date: 25 May 2016

Accepted date: 4 August 2017

Please cite this article as: Jung S., Song S., Chang M., Park S. Range image registration based on 2D synthetic images. *Computer-Aided Design* (2017), <http://dx.doi.org/10.1016/j.cad.2017.08.001>

This is a PDF file of an unedited manuscript that has been accepted for publication. As a service to our customers we are providing this early version of the manuscript. The manuscript will undergo copyediting, typesetting, and review of the resulting proof before it is published in its final form. Please note that during the production process errors may be discovered which could affect the content, and all legal disclaimers that apply to the journal pertain.

\*Highlights (for review)

## Highlights

- Registration procedure of 3D range images based on 2D synthetic images
- Risk minimization of the original ICP, getting stuck in a local minimum
- 2D synthetic image generation by varying orientations and resolutions
- A 2D registration method (SURF) has been adapted to 3D registration
- Experimental results show that the proposed procedure outperforms existing methods

\*Manuscript  
[Click here to view linked References](#)

## Range Image Registration based on 2D Synthetic Images

Sukwoo Jung, Seunghyun Song, Minho Chang\*  
Department of Mechanical Engineering, Korea University  
Anam-dong, Seongbuk-gu, Seoul, Korea  
Sangchul Park  
Department of Industrial Engineering, Ajou University  
Woncheon-dong, Yeongtong-gu, Suwon, Korea

**Abstract:** Proposed in this paper is a new procedure of range image (point cloud) registration reducing the risk of the original Iterative Closest Point (ICP) algorithm which gets stuck in a local minimum. To reduce this risk, it is essential to achieve the fine initial alignment of the given range images. The proposed procedure employs a 2D image registration method to achieve the fine initial alignment instead of a 3D feature based registration method. Although the 2D image registration method has also the risk of mismatching, we minimize the risk by increasing the number of test cases and selecting the answer that gains the most votes. To generate effective test cases, multiple 2D images are synthetized from the given range images by varying the orientation and resolution. The proposed procedure is implemented and tested for various examples, with experimental results showing that it outperforms existing methods.

**Key words:** range image, 3D registration, image registration, scanning, initial alignment, ICP

---

\*Correspondence: Minho Chang ([mhchang@korea.ac.kr](mailto:mhchang@korea.ac.kr))  
Professor, Department of ME, Korea University  
Anam-dong, Seongbuk-gu, Korea

## 1. INTRODUCTION

A 3D scanner is a device to create a point cloud data by scanning a real-world object. The collected point clouds can then be used to generate a 3D digital model in a process called reconstruction. Although there is a variety of technologies available for acquiring the shape of a real-world object, Structured Light Systems (SLS) are currently most popular due to their fast measuring speed, simple optical arrangement, non-contact measurement, moderate accuracy, low cost, and ability to function under varying ambient light conditions [1, 4, 6, 14, 36]. Figure 1 shows a general configuration of an SLS consisting of a projector and cameras. The projector illuminates the object with a structured light source, and the cameras capture the scene to produce 3D range image. The range image can be considered as a point cloud containing the spatial coordinates for the surface points of the object.

❖ Figure 1. Configuration of a structured light system ❖

Since a SLS can measure only the area visible from a specific scanning orientation, the full reconstruction of a real-world object requires three major steps: 1) acquiring multiple range images from different viewpoints to cover the entire surface area of the given object, 2) applying a 3D registration process to the acquired range images, and 3) merging the multiple range images to generate a 3D digital model. This paper is focusing on the second step, the registration of range images, of which the accuracy is very important to ensure the quality of the reconstructed 3D model.

The most common method for 3D registration is the well-known Iterative Closest Point (ICP) algorithm [2], which minimizes the distance between two point clouds. The ICP algorithm works for a pair of point clouds, a target and a source. The target point cloud is kept fixed, while the source point cloud is transformed (with a combination of translation and rotation) to minimize the distance between them.

The original ICP algorithm [2] sets the closest points as the correspondence and optimizes the root mean squared deviations. Chen [3] employed point-plane distance by

estimating the normal vectors of the point clouds. Ever since then, there have been various researches on the ICP algorithm [5], and they can be roughly categorized into five groups: improving computing speed through efficient correspondence detection [7, 8, 18, 19, 20, 21], improving accuracy by defining the appropriate energy function [9, 10, 12, 23, 25, 38], combining existing algorithms [13, 16, 17], finding correspondence by using probability [25, 26, 29], and eliminating correspondence outliers [11, 15].

Although the ICP algorithm usually offers good results, it has the risk of becoming stuck in a local minimum, especially in cases where there is only a rough initial alignment between the target and the source point clouds. As shown in Figure 2(a), the ICP algorithm works well when the two point clouds are within an acceptable range in terms of their position and orientation. The ICP algorithm can become stuck in a local minimum, however, if the two point clouds are outside this acceptable range, as shown in Figure 2(b).

#### ⤵ Figure 2. Limitation of the ICP algorithm ⤵

To overcome this problem, many researchers have investigated methods to achieve the fine initial alignment of the two point clouds [22]. Most have focused on the use of 3D features in the given point clouds. Previous research on initial alignment can be classified by the type of 3D feature used: curves [24, 37], feature histograms (FPFH) [27], 4-point congruent sets [28], and spin images [32]. Nevertheless, these initial alignment methods using 3D features may not generate useful results when the scanned data has occlusions or a consistent curved geometry such as a cylinder or a cube.

As the relationship between a 2D image and a 3D point cloud can be obtained, the matching relations of 2D features can be used to achieve the initial alignment. Since 2D image registration methods [34, 35] use only the texture and the intensity of the image for calculations, they are much faster than 3D registration and can find 2D features robustly. From this reason, some authors proposed the method using 2D images in 3D

registration [41, 42]. However, these methods perform poorly if the viewpoint of the camera moves beyond the threshold degree, because the scene, the geometry, and the intensity of the image changes. Moreover, the algorithm can only perform on a flat and textured surface. This is one of the fundamental problems of 2D image registration algorithms. Therefore, there always exists a risk that registration may return incorrect matching relations, and currently no solution has been found that can eliminate this problem completely.

The objective of this paper is to develop a new registration procedure that minimizes the risk faced by the original ICP algorithm, that of becoming stuck in a local minimum. To reduce this risk, it is necessary to achieve the fine initial alignment of the range images. Our approach is to reduce the risk of using 2D registration by generating multiple pairs of synthetic images from the given range images by changing their resolution and orientation in order to obtain a large number of test cases. Each pair contains two synthetic images, one from the source range image and the other from the target range image. For each pair of 2D synthetic images, we can obtain matching relations using the 2D registration. The proposed approach selects the matching relations which obtain the most votes from the multiple pairs of 2D synthetic images.

⤵ Figure 3. The approach of proposed 3D registration algorithm based on 2D image registration ⤵

As shown in Figure 3, the proposed registration procedure consists of five steps: 1) synthetizing a 2D image set from both the target range image and the source range image, 2) applying 2D registration to the test cases, each of which is a pair of synthetic images, one from the target image set and the other from the source image set, 3) finding the matching relations that obtain the most votes from the test cases and removing the outliers, 4) transforming the source range image to achieve fine initial alignment, and 5) applying the ICP algorithm to the aligned range images.

The remainder of this paper is organized as follows. Section 2 addresses the proposed approach to the fine initial alignment of given range images with image registration. Section 3 describes the details and the overall procedure of the proposed algorithm, and Section 4 shows the results of the experimentation. Finally, concluding remarks are given in Section 5.

## 2. APPROACH TO THE FINE INITIAL ALIGNMENT OF RANGE IMAGES WITH IMAGE REGISTRATION

As mentioned earlier, initial alignment algorithms work on two range images (a target point cloud and a source point cloud). Since a range image is generated from 2D images from an SLS, the correspondence between a 2D image pixel and a 3D point cloud vertex can be obtained. Therefore, 2D image registration can be used to achieve the initial alignment of the 3D data. The 2D image registration algorithm works on two given images (a source image and a target image), and consists of two major steps: 1) finding two sets of interesting points from both images using the detector, and 2) finding matching relations between the interesting points using the descriptor. This matching relations can be used to calculate the transformation matrix for the initial alignment. One of the most popular 2D image registration methods is the well-known Speed Up Robust Features (SURF) algorithm [30]. SURF is based on rotation invariant features and is known to be efficient. The proposed approach employs SURF to find the correspondence between the 2D images (the source image and the target image). However, the reliability of SURF is weakened when the viewpoint changes between images, a fundamental problem of the 2D image registration algorithms.

In SURF, a Hessian corner detector is used to calculate the interesting points. The pixels with a value above the minimum threshold are considered interesting points. We set this variable to 400 [45]. Figure 4(a) displays the interesting points according to the SURF detector. The center of the circle is an interesting point location, and the radius of

the circle indicates the value of the feature point. Figure 4(b) presents the matching relations resulting from SURF descriptor matching. As mentioned above, the results from SURF may be incorrect if the viewpoint of the camera moves beyond a certain threshold.

❖ Figure 4. Examples of incorrect SURF matches ❖

Although there are many algorithms differ in defining the detector and descriptor, their registration results are not much better than that of SURF [39, 43]. Therefore, we have not defined a new detector or descriptor. Instead, this research focuses on finding good matches with the given interesting points and a given descriptor. If the interesting point sets are fixed, the matching relations are affected by the descriptor, which is calculated from the image. Consequently, we propose that we can extract good matching relations by generating multiple different matching relations with many similar images and selecting the matching relations with the most votes. In this paper, similar 2D images are created in two ways: 1) using a 3D point cloud to generate 2D synthetic images from different viewpoints, and 2) using a 2D image to make resized images that have different resolutions.

Since the 2D image registration algorithm is weakened by changes in the viewpoint of the images, registration performance can be improved if the viewpoint difference between two images is reduced. The ASIFT [31] algorithm, which applies an arbitrary affine transformation matrix to an image, is employing this approach. Utilizing the 3D point cloud data, the proposed procedure can derive more realistic synthetic images that are similar to the real-world object. When transforming a range image to a different viewpoint, there are three pivot axes around which the camera can rotate (Figure 5). The movement along x-axis means the horizontal viewpoint change, y-axis the vertical viewpoint change, and z-axis the 2D image plane rotation. Since the SURF is insensitive to 2D image rotation, z-axis rotation can be ignored and the proposed

procedure rotates the point cloud along the x-axis and y-axis. The rotation for each axis has three conditions: clockwise rotation, counterclockwise rotation, and remaining still. That is the reason why the proposed algorithm uses 9 ( $=3*3$ ) synthetic images from the different orientations.

❖ Figure 5. The rotational axes used in transforming the range image ❖

After creating the synthetic images for the different orientations, the proposed procedure then generates synthetic images of different resolutions. When the resolution of the image is reduced, the features of an image become clearer. Meanwhile, a high resolution image has more detailed features and information than a low resolution image [44]. Therefore, the proposed algorithm uses three different resolution images (high, medium, and low) for image registration to generate better results.

❖ Figure 6. 2D synthetic image set generation from a range image ❖

Normally, 2D image registration algorithms, including SURF, use two images; a source image and a target image. The proposed method, in contrast, uses many similar images generated from the point cloud data (Figure 6): 9 transformed synthetic images are generated from the different orientations, and 3 synthetic images of differing resolutions generated for each of the 9 transformed synthetic images. This give a total of 27 images each for the source and the target data. An image pair is formed with two images of the same resolution, one from the source image set and the other from the target image set. Therefore, the proposed algorithm calculates the matching relations from 243 ( $=9*9*3$ ) image pairs. As the proposed method selects the matching relations that overlap the most from these 243 test cases, the registration results are robust to the viewpoint changes and resizing.

The benefit of the proposed 2D registration method is that it can be applied to various image registration algorithms to improve the results. In addition, the number of different orientation images and different resolution images can be modified for

computational efficiency or registration accuracy.

### 3. PROPOSED 3D REGISTRATION ALGORITHM

To generate the synthetic images from the different orientations, the back-projection method is used. As the calibration information of the camera is known, the correspondence between the point cloud vertex and the image pixels can be obtained from back-projection. In the back-projection of the 3D point cloud to the image plane, formulas (1) and (2) are used.

$$\begin{aligned} u &= \frac{f_x \cdot x}{z} + c_x \quad (1) \\ v &= \frac{f_y \cdot y}{z} + c_y \quad (2), \end{aligned}$$

where  $u$  and  $v$  are the coordinates of the image plane (pixels), and  $x$ ,  $y$  and  $z$  are the Cartesian coordinates of the point cloud (vertices).  $f_x$  and  $f_y$  are the focal lengths of the camera, and  $c_x$  and  $c_y$  are the principal axes of the camera.

Applying the above formula to the transformed range image, synthetic images from the different orientations can be generated. The 2D-3D relationship between the data and back-projected synthetic images are shown in Figure 7.

❖ Figure 7. The relationship between the 2D-3D data and the back-projected synthetic images ❖

The process of creating synthetic images from the different orientations is as follows: 1) transform the 3D point cloud data to a different viewpoint with a transformation matrix, 2) obtain the synthetic image using back-projection of the 3D point cloud to the image plane with formulas (1) and (2), 3) fill the intensity value of the synthetic image by referring to the texture information of the original 2D image, 4) apply a hole-filling algorithm[40] to fix holes in the synthetic image that are formed by the transformation of a sparse 3D surface. The hole-filling algorithm detects holes and fills them using the interpolation of neighboring pixels. Figure 8 shows an example of

the synthetic images from the 9 different orientations. Figure 8(a) shows the synthetic images of the source point cloud, and Figure 8(b) the synthetic images of the target point cloud.

 Figure 8. Synthetic image generation from 9 different orientations 

After generating the transformed synthetic images, the proposed algorithm creates 3 different resolution images for each synthetic image. The downsized image is generated using the simple uniform sampling method. Since there are 3 different resolution images for 9 different orientation images, 27 synthetic images are generated; these are considered one image set for the range image in the proposed method.

As previously mentioned, an image pair is formed between two images with the same resolution: one from the source image set and the other from the target image set. When 2D image registration is applied to the 243 image pairs, each image pair produces different matching relations. The interesting points in each matching relation set are originated from the one image pair and projected to the other image plane. For each of the interesting points, we count the number of overlapping matching relation sets and select the most voted points. These matching points that frequently overlap can be considered highly reliable correspondences. The matching points that overlaps less than the threshold are removed from the correspondence. consequently, selecting the most commonly occurring matching relations may reduce the risk of selecting mismatched points and thus improve the registration results.

Finding the matching relations from the multiple image pairs is summarized as follows:

- (1) Use a detector to obtain the interesting points from the source (target) image.
- (2) Transform the range image and back-project it to the image planes, generating synthetic images of various orientations. Use the same transformation matrix and projection matrix to convert the interesting points in each image plane.

(3) Resize the images obtained from (2) to generate synthetic images of various resolutions. Convert the interesting points of (1) in the resized images using interpolation. The synthetic images generated by (2) and (3) from the source (target) range image are together taken to be the source (target) image set.

(4) Calculate the descriptor of interesting points for each synthetic image.

(5) Obtain the matching relations of image pairs with the same resolution, one from the target image set and the other from the source image set. The Mahalanobis distance of the descriptors from the two images are calculated and the closest points are defined as a matching relation.

6) Consider all of the matching relations obtained from (5), and select the ones that receive the votes over the threshold.

Figure 9 shows an example of matching relations from multiple synthetic image pairs. Figure 9(a) is the matching relation sets of multiple image pairs. The matching relations that obtain the most votes from these matching relation sets are shown in Figure 9(b).

⤵ Figure 9. Finding matching relations from multiple image pairs ⤵

In this research, the proposed procedure uses 27 images each on the source and target data. As it selects the most commonly occurring correspondences from the 243 matching relation sets, the proposed method is robust to viewpoint changes and resizing. Even though the algorithm uses numerous images, the elapsed calculation time for the proposed method is not impractical because the algorithm uses only one set of interesting points. Because the most time-consuming step of 2D registration is finding interesting points with the detector, the proposed algorithm has an acceptable computational cost.

We generated the synthetic images with 10 degrees of rotations for each axes. The resolutions of the images we used were 1280 \* 960, 1024 \* 768, and 768 \* 576. From these settings, the proposed 2D registration algorithm normally finds dozens of

matching relations. At least 3 correct correspondences are required to generate a transformation matrix. Thus, to find more than 3 correct correspondences from all of the matching relations, we use the Random Sample Consensus (RANSAC) [33] technique.

RANSAC is an algorithm commonly used to eliminate outliers. When performing RANSAC with ICP, data sets of tens of thousands of points are typically used. Even if this data is down-sampled, ICP data sets still use thousands of points. Performing RANSAC iteratively increases the computational cost of ICP. In contrary, the proposed method uses only dozens of points. Therefore, the computational cost of using RANSAC in the proposed method is substantially lower than that of ICP. The proposed method thus uses RANSAC to sort out the correct correspondences quickly and precisely.

After the correct corresponding points have been selected, a transformation matrix is calculated with singular value decomposition and the linear least-squares method. This transformation matrix is the initial alignment for 3D registration. We then used ICP for the fine 3D registration.

The overall process for the algorithm can be written in pseudo-code as follows:

**The overall process of the proposed algorithm in pseudo-code:**

```
// Input:  
//  $P_s, P_t$  : the source point cloud, the target point cloud,  
//  $I_{s0}^0, I_{t0}^0$  : the source image, the target image,  
//  $\mathbf{R}$  : the back-projection matrix of the data  
  
// Output:  
//  $T_f$  : the final transformation matrix to align the source point cloud to the target point  
cloud  
  
// Main Variables:  
//  $D_s^0, D_t^0$  : interesting points from SURF detector in the source and the target image,  
//  $T_s^n, T_t^n$  : specific transformation matrix to generate the synthetic image,  
//  $I_{sm}^n, I_{tm}^n$  : synthetic image set for the source and the target data,
```

```

//  $r_m$  : specific resolution to generate the synthetic image,
//  $M$  : entire matching relations,
//  $M_c$  : correct correspondences

Step 1) Synthetic image set generation
     $D_s^0, D_t^0 \leftarrow$  interesting points from SURF detector
    for (the number of orientation varying images  $n = 0 ; n < n_{max} ; n++$ )
         $\{I_{s0}^n, I_{t0}^n, D_{s0}^n, D_{t0}^n\} \leftarrow \{T_s^n P_s R, T_t^n P_t R, T_s^n D_s^0, T_t^n D_t^0\}$ 
        for (the number of resolution varying images  $m = 0 ; m < m_{max} ; m++$ )
             $\{I_{sm}^n, I_{tm}^n\} \leftarrow \{\text{resize}(I_{sm}^n, r_m), \text{resize}(I_{tm}^n, r_m)\}$ 
             $\{D_{sm}^n, D_{tm}^n\} \leftarrow \{\text{interpolate}(D_{sm}^n, r_m), \text{interpolate}(D_{tm}^n, r_m)\}$ 
        end
    end

Step 2) Find the matching relation sets from multiple image pairs using the SURF
descriptor
    for (the number of orientation variation  $n_1 = 0 ; n_1 < n_{max} ; n_1++$ )
        for (the number of orientation variation  $n_2 = 0 ; n_2 < n_{max} ; n_2++$ )
            for (the number of resolution variation  $m = 0 ; m < m_{max} ; m++$ )
                 $\{M_m^{n_1, n_2}\} \leftarrow \text{SURF\_match}(I_{sm}^{n_1}, D_{sm}^{n_1}, I_{tm}^{n_2}, D_{tm}^{n_2})$ 
                 $\{M\} \leftarrow M_m^{n_1, n_2}$ 
            end
        end
    end

Step 3) Select the most commonly occurring matching relations and remove the outliers
     $\{M\} \leftarrow \text{most\_voted}(M)$ 
     $\{M_c\} \leftarrow \text{RANSAC}(M)$ 

Step 4) Initial alignment
     $\{T_{init}\} \leftarrow \text{min dist}(M_c)$ 

Step 5) Fine tuning with ICP
     $\{T_f\} \leftarrow \text{ICP}(T_{init} \cdot P_s, P_t)$ 

```

The first step is generating the 2D synthetic image set. The interesting points ( $D_s^0, D_t^0$ ) for each source and target image are calculated using a SURF detector. The

synthetic images of orientation variations ( $I_{s0}^n, I_{t0}^n$ ) resolution variations ( $I_{sm}^n, I_{tm}^n$ ) can then be generated. The corresponding interesting points in the synthetic images of orientation difference ( $D_{s0}^n, D_{t0}^n$ ) are calculated using the given transformation matrix ( $T_s^n, T_t^n$ ). The corresponding interesting points in the synthetic images of resolution difference ( $D_{sm}^n, D_{tm}^n$ ) are obtained by interpolation.

Next, the matching relations set with multiple 2D image pairs is calculated. The pairs of two images with the same resolution, one from the source image set and the other from the target image set, are generated. Then the matching relations of each image pair are obtained with SURF descriptor matching.

After collecting all the matching relations ( $M$ ), the next step is to extract the matching relations with the most votes and use RANSAC to sort out the correct correspondences( $M_c$ ). To obtain the initial alignment transformation matrix ( $T_{init}$ ) with the correct correspondences, we minimize the point-to-plane distance metric using formula (3).

$$\arg \min \sum_i^{\text{size of } M_c} \|(T_{init}v_i^s - v_i^t) \cdot n_i^t\|^2 \quad (3),$$

where  $v_i^s$  is the source point cloud  $i$ -th vertex,  $v_i^t$  is the target point cloud  $i$ -th vertex, and  $n_i^t$  is the target point cloud  $i$ -th normal vector.

Finally, after the initial alignment, ICP is applied to find the final transformation matrix ( $T_f$ ). An overview of the proposed registration process is shown in Figure 10.

❖ Figure 10. Overview of the proposed registration process ❖

As we mentioned earlier, the number synthetic images can be modified for computational efficiency or registration accuracy. Table 1 shows the computational elapsed time and the ratio of the correct matching points according to the number of images used in the algorithm. The algorithm was tested with the teeth model shown above. As the number of images increases, the correct matching points ratio increases. We used 27 images for better performance of the proposed algorithm. The optimal

number of images can be varied according to the tested object and the user environment.

[Table 1] Performance and computation time according to the number of images

| Number of Images | Elapsed time (sec) | Correct matching point ratio (%) |
|------------------|--------------------|----------------------------------|
| 3                | 1.54               | 1.5                              |
| 6                | 1.95               | 3.7                              |
| 9                | 2.06               | 6.3                              |
| 12               | 2.38               | 6.6                              |
| 15               | 2.51               | 7.8                              |
| 18               | 2.78               | 8.5                              |
| 21               | 2.96               | 9.1                              |
| 24               | 3.01               | 9.5                              |
| 27               | 3.10               | 9.7                              |

In the next section, experimental results comparing the proposed algorithm to other well-known methods are described.

#### 4. EXPERIMENTS AND RESULTS

##### 4.1 Experiment Set-up

The proposed algorithm was implemented in C++ language and test runs were made on a personal computer with an i5-2500 processor with 8 GB memory and a Windows 7 operating system. For the experimentation, we used the commercial scanner REXCAN4® developed by Medit. As shown in Figure 11, three models were used for the experiments: a teeth model, a dinosaur model, and a mechanical part.

❖ Figure 11. The real-world objects used in the experiments ❖

In the experiment, we compared the proposed algorithm with the existing algorithms FPFH [27], ICPIF [24], SURF [34] and ICP [3]. FPFH and ICPIF represent 3D feature-based registration algorithms, and SURF is an image-based algorithm using an existing 2D registration method. As ICP is a commonly used algorithm, we also

compared it with the proposed algorithm. In the experiment, we measured the elapsed time, root mean square deviations (RMSD) of the results, and success or failure of registration. Registration was performed with all of the data sets we obtained, and the possible registration ranges (the maximum difference of two data that the algorithm perform registration successfully) of each algorithm were analyzed.

#### 4.2 Registration of range images with translational variations

We compare the performance of the algorithms in the presence of translational movement. The object was moved horizontally by 100 pixels and 11 data sets were obtained. Figure 12 shows the results of the experiment. The x-axis is the translational movement (pixel), and the y-axis is the root mean square deviations (mm). As shown in the graph, the proposed method and FPFH were successful in registration for every data set, followed by the SURF, ICPIF, and ICP. Theoretically, SURF should also succeed in the registration of all data because 2D feature based image registration is translational invariant. However, the experimental results show that SURF fails if the data set moves more than 800 pixels. This is because the object was scanned from different positions, and the scanned data has different 3D point cloud data, although they look almost identical in the image. Nevertheless, SURF is far better than ICP because the 2D images are stable in the translational movements. The proposed method, which is a 2D image based algorithm, also shows an outstanding performance in the translational movement.

❖ Figure 12. RMSD of the fine registration results using the tested algorithms (translational variation) ❖

#### 4.3 Registration of range images with rotational variations

We also analyzed the performance of the algorithms in the presence of rotational movement. The objects were scanned from the various viewpoints on the hemispheric

surface (Figure 13). The viewpoints were rotated 10 degrees horizontally and vertically, leading to 360 data sets.

❖ Figure 13. 3D data acquisition on a hemispheric surface ❖

To analyze the registration range for the rotational movement, the registration algorithms were tested for all of two point clouds in the same row. The algorithms were performed with  $10*36*35 = 12600$  data sets and the results were sorted with the angle difference of the two point clouds. Figure 14 displays the experimental results for initial alignment using the tested algorithms. Figure 15 presents the experimental results for the fine registration using the tested algorithms. The x-axis is the rotational angle difference (degree), and the y-axis is the root mean square deviations (mm). As clearly shown in the two figures, initial alignment critically affects the fine registration results. The proposed method exhibited the largest registration range with approximately 73 degrees, followed by FPFH (53 degrees), ICPIF (26 degrees), SURF (20 degrees), and ICP (20 degrees). The reason why the proposed method has the largest registration range is that it uses synthetic images of different orientations and resolutions to obtain robust matching points of 2D features.

❖ Figure 14. RMSD of the initial alignment results using the tested algorithms  
(rotational variation) ❖

❖ Figure 15. RMSD of the fine registration results using the tested algorithms  
(rotational variation) ❖

We also tested the registration performance with two point clouds in other rows. We performed the registration algorithms with the center positioned point cloud and the surrounding point clouds. Figure 16 shows the image data sets and the registration range of the algorithms in colored boxes. The proposed method is in red, SURF blue, ICPIF purple, FPFH green, and ICP orange.

Figure 16. Rotational variation data set images and registration range of the tested algorithms

The vertical registration range is smaller than the horizontal one. It seems that the scanned objects have many features on the front side rather than the upper side. Nevertheless, the proposed algorithm has larger coverage of registration range than the other algorithms. Table 2 shows the average elapsed time and registration range for the tested algorithms.

[Table 2] Performance of the tested algorithms

| Algorithm                                | Proposed Method | SURF | ICPIF | FPFH  | ICP  |
|--|-----------------|------|-------|-------|------|
| Elapsed time (sec)                       | 5.17            | 3.55 | 7.89  | 10.58 | 2.02 |
| Translational registration range (pixel) | 1000            | 700  | 467   | 1000  | 368  |
| Rotational registration range (degree)   | 73°             | 20°  | 26°   | 53°   | 20°  |

## 5. SUMMARY

In this research, a new registration procedure for the range images acquired by an optical 3D scanner is proposed. Since registration has a significant impact on the quality of a reconstructed CAD model, it is essential to ensure the stability of the registration algorithm. One of the major attributes of the proposed procedure is that it minimizes the major risk of the original ICP algorithm, becoming stuck at a local minimum, by achieving the fine initial alignment of the range images. For the initial alignment, we employ a 2D image registration method instead of using a 3D feature based method. Since 2D image registration methods use only texture and intensity to calculate 2D features, they are much faster than 3D registration methods. Although 2D image registration also runs the risk of mismatches, we minimize this risk by increasing the number of test cases (using synthetic images) and selecting the answers obtaining the

most votes.

The proposed registration procedure consists of five steps: 1) 2D synthetic image set generation from both the target range image and the source range image, 2) finding the matching relation sets from each image pair using the SURF descriptor, 3) selecting the matching relations which obtain the most votes from multiple image pairs and removing the outliers, 4) transforming the source range image to achieve fine initial alignment, and 5) applying the ICP algorithm to the initially aligned range images. The SURF algorithm used in the proposed procedure can be replaced with other 2D registration algorithms for different results. The number of images can also be increased to enhance registration accuracy or decreased for computational efficiency.

The proposed procedure has been implemented, and was compared with the existing methods FPFH, ICPIF, SURF, and ICP. Experimentation shows that the proposed approach provides better registration results and is more stable (robust) compared to the existing methods in terms of both rotational and translational movement. This is because the proposed algorithm uses synthetic images of different orientations and resolutions to obtain robust matching points of 2D features. In addition, the computation time of the proposed approach is faster than that of FPFH and ICPIF because we employ 2D feature based method instead of 3D feature based registration method.

However, the proposed algorithm handles too many images to perform fast registration. Further research and optimization is needed to use the algorithm in real-time applications.

## ACKNOWLEDGEMENT

This research was supported by the Technology Innovation Program (10065150, Development of Low-cost and Small LIDAR System Technology based on 3D Laser

scanning for 360 Real-time Monitoring), funded by the Ministry of Trade, Industry & Energy (MOTIE, Korea) and the Korea Evaluation Institute of Industrial Technology (KEIT, Korea). This work was also partially supported by National Research Foundation (NRF-2015R1A2A2A01005871) by the Ministry of Education, Science and Technology, Korea.

## REFERENCES

1. Minho Chang, Sang C Park. Reverse engineering of a symmetric object, *Computers & Industrial Engineering*, 2008;55(2):311-320
2. P J Besl, N D McKay. A method for registration of 3D shapes, *IEEE Transactions on Pattern Analysis and Machine Intelligence*, 1992;14(2):239-256.
3. Y Chen, G Medioni. Object modeling by registration of multiple range views, *Image and Vision Computing*, 1992;10(3):145-155.
4. Minho Chang, Sang C Park. Automated scanning of dental impressions, *Computer-Aided Design*, 2009;41(6):404-411.
5. S Rusinkiewicz, M Levoy. Efficient variants of the ICP algorithm, *Proceedings of the 3-D Digital Imaging and Modeling*, May 2001:145-152.
6. Sang C Park, Minho Chang. Reverse engineering with a structured light system, *Computer & Industrial Engineering*, 2009;57(4):1377-1384
7. R Benjamaa, F Schmitt. Fast global registration of 3D sampled surfaces using a multi-z-buffer technique, *Image and Vision Computing*, 1999;17(2):113-123.
8. SY Park, M Subbarao. An accurate and fast point-to-plane registration technique, *Pattern Recognition Letters*, 2003;24(16):2967-2976.
9. S Ying, J Peng, S Du, H Qiao. A scale stretch method based on ICP for 3D data registration, *IEEE Transactions on Automation Science and Engineering*, 2009;6(3):559-565.
10. L Zhang, SI Choi. Robust ICP registration using biunique correspondence, *International Conference on 3D Imaging, Modeling, Processing, Visualization and Transmission*, May 2011:80-85.
11. JM Phillips, R Liu, C Tomasi. Outlier robust ICP for minimizing fractional RMSD,

- International Conference on 3D Digital Imaging and Modeling, Aug 2007:426-434.
12. T Zinber, J Schmidt, H Niemann. Point set registration with integrated scale estimation, International Conference on Pattern Recognition and Image Processing, 2005:116-119.
  13. H Pottmann, S Leopoldseder, M Hofer. Registration without ICP, Computer Vision and Image Understanding, 2004;95(1):54-71.
  14. Minho Chang, JW Oh, Sang C Park. Next viewing directions for the scanning of dental impressions, Computer-Aided Design, 2015;66:24-32.
  15. P Krsek, T Pajdla, V Hlavac, R Martin. Range image registration driven by a hierarchy of surface differential features, In: 22<sup>nd</sup> Workshop of the Austrian Association for Pattern Recognition, 1998:175-183.
  16. A V Segal, D Haehnel, S Thrun. Generalized-ICP, Robotics: Science and Systems, 2009.
  17. N J Mitra, N Gelfand, H Pottmann, L Guibas. Registration of point cloud data from a geometric optimization perspective, Proceedings of the 2004 Eurographics/ACM SIGGRAPH Symposium on Geometry Processing, July 2004:22-31
  18. SY Park, SI Choi, J Kim, JS Chae. Real-time 3D registration using GPU, Machine Vision and Applications, 2011;22(5):837-850.
  19. A Nuchter, K Lingemann, J Hertzberg. Cached k-d tree search for ICP algorithms, International Conference on 3D Digital Imaging and Modeling, 2007:419-426.
  20. S Leopoldseder, H Pottmann, H Zhao. The  $d^2$ -Tree: A hierarchical representation of the squared distance function, Technical Report 101, Vienna University of Technolohgy, 2003.
  21. D Qiu, S May, A Nuchter. GPU-accelerated nearset neighbor search for 3D registration, International Conference on Computer Vision Systems, 2009:194-203.
  22. G K L Tam, Z Q Cheng, Y K Lai, F C Langbein, Y Liu, D Marshall, R R Martin, X F Sun, P L Rosin. Registration of 3D point clouds and meshes: A survey from rigid to non-rigid, IEEE Transactions on Visualization and Computer Graphics, 2013;19(7):1199-1217
  23. D F Huber, M Herbert. Fully automatic registration of multiple 3D data sets, Image and Vision Computing, 2003;21(7):637-650.
  24. X Li, I Guskov. Multi-scale features for approximate alignment of point-based

surfaces, Proceedings of the third Eurographics SIGGRAPH Symposium on Geometry Processing, 2005.

25. Y Liu. Automatic 3D free form shape matching using the graduated assignment algorithm, Pattern Recognition, 2005;38(10):1615-1631.
26. S Granger, X Pennec. Multi-scale EM-ICP: A fast and robust approach for surface registration, Computer Vision ECCV, 2002;2353:418-432.
27. R B Rusu, N Blodow, M Beetz. Fast point feature histograms (FPFH) for 3D registration, IEEE International Conference on Robotics and Automation, 2009:1845-1853.
28. D Aiger, N J Mitra, D Cohen-Or. 4-Points congruent sets robust pairwise surface registration, ACM Transactions on Graphics (Proc. SIGGRAPH), 2008;27(3):1-10.
29. A Myronenko, X Song. Point set registration: Coherent point drift, IEEE Transactions on Pattern Analysis and Machine Intelligence, 2010;32(12):2262-2275.
30. H Bay, A Ess, T Tuytelaars, L V Gool. SURF:Speeded up robust features, Computer Vision and Image Understanding, 2008;110(3):346-359.
31. J M Morel, G Yu. ASIFT: A new framework for fully affine invariant image comparison, SIAM Journal on Imaging Sciences, 2009;2(2):438-469.
32. A E Johnson, M Hebert. Using spin images for efficient object recognition in cluttered 3D scenes, IEEE Transactions on Pattern Analysis and Machine Intelligence, 1999;21(5):433-449.
33. M Fischler, R Bolles. Random sample consensus: A paradigm for model fitting with applications to image analysis and automated cartography, Communications of the ACM, 1981;24(6):381-395.
34. B Zitova, J Flusser. Image registration methods: A survey, Image and Vision Computing, 2003;21(11):977-1000.
35. D G Lowe. Object recognition from local scale-invariant features, Computer Vision, 1999;2:1150-1157.
36. T Kim, Y Seo, S Lee, Z Yang, M Chang. Simultaneous registration of multiple views with markers, Computer-Aided Design, 2009;41(4):231-239.
37. E Kalogerakis, D Nowrouzezahrai, P Simari. Extracting lines of curvature from noisy point clouds, Computer-Aided Design, 2009;41(4):282-292.

38. TM Tucker, TR Kurfess. Newton methods for parametric surface registration. Part I. Theory, Computer-Aided Design, 2003;35(1):107-114.
39. E Rublee, V Rabaud, K Konolige, G Bradski. ORB: an efficient alternative to SIFT or SURF, Computer Vision, 2011;2564-2571.
40. KJ Oh, S Yea, YS Ho. Hole filling method using depth based in-painting for view synthesis in free viewpoint television and 3-D video, Picture Coding Symposium, 2009
41. Henry P, Krainin M, Herbst E, Ren X, Fox D. RGB-D mapping: Using Kinect-style depth cameras for dense 3D modeling of indoor environments, The International Journal of Robotics Research, 2012;31(5), 647-663.
42. Bendels G, Degener P, Wahl R, Koertgen M, Klein R. Image-based registration of 3D-range data using feature surface elements, The 5th International Symposium of Virtual Reality, Archaeology and Cultural Heritage, VAST, 2004.
43. Christoffer V, Achim JL. SIFT, SURF and seasons: Long-term outdoor localization using local features, In Proceedings of the European Conference on Mobile Robots, 2007;253-258.
44. R. Appel, S. Belongie, P. Perona, and P. Doll. Fast Feature Pyramids for Object Detection, IEEE Transaction on Pattern Analysis Machine Intelligence, 2014;36(8),1–14.
45. R. Grycuk, M. Gabryel, M. Korytkowski, R. Scherer. Content-based Image Indexing by Data Clustering and Inverse Document Frequency, International Conference: Beyond Databases, Architectures and Structures, 2014;374-383

Figure

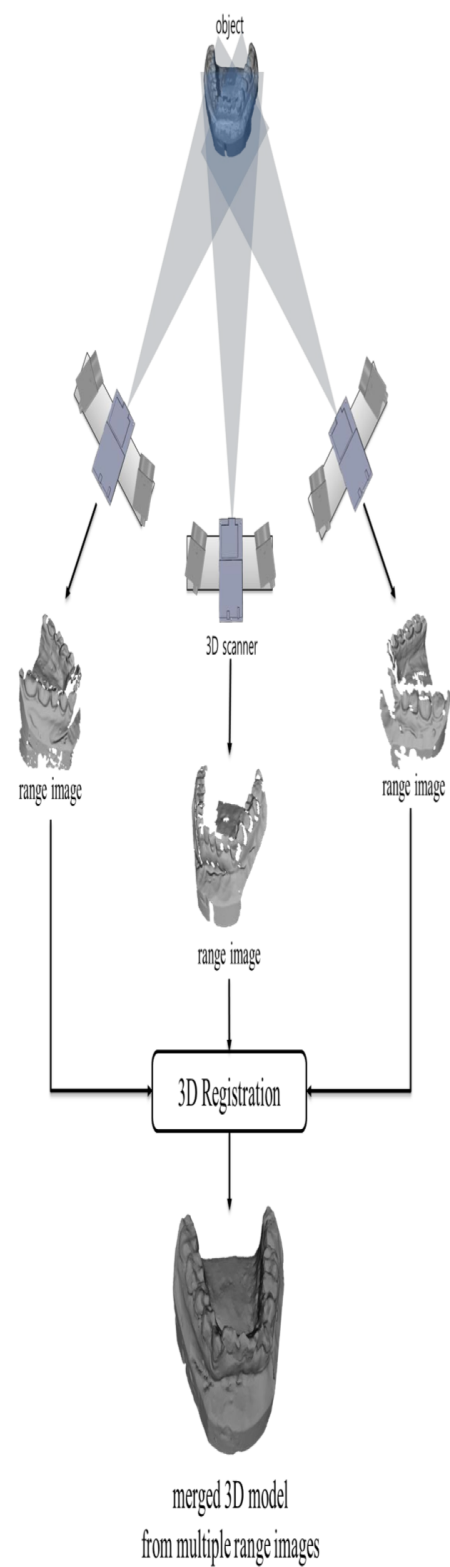
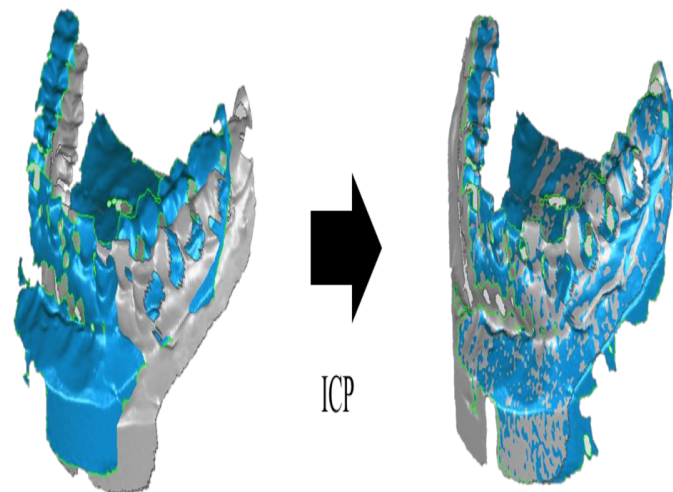
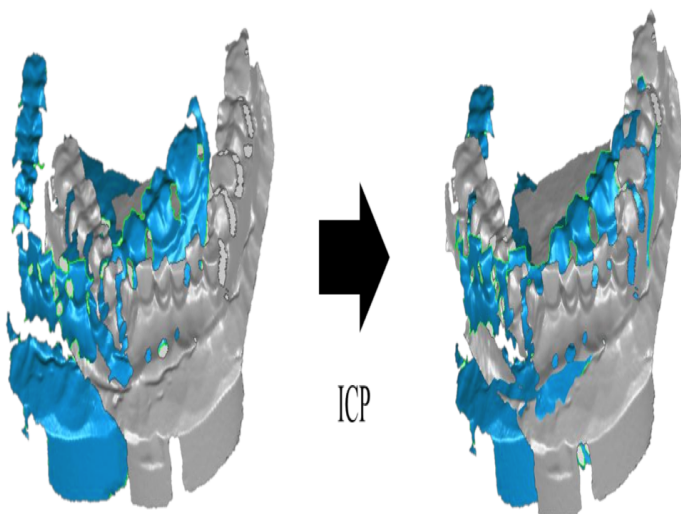


Figure 1. Configuration of a structured light system



(a) ICP with fine initial alignment



(b) ICP with rough initial alignment (local minimum)

Figure 2. Limitation of the ICP algorithm

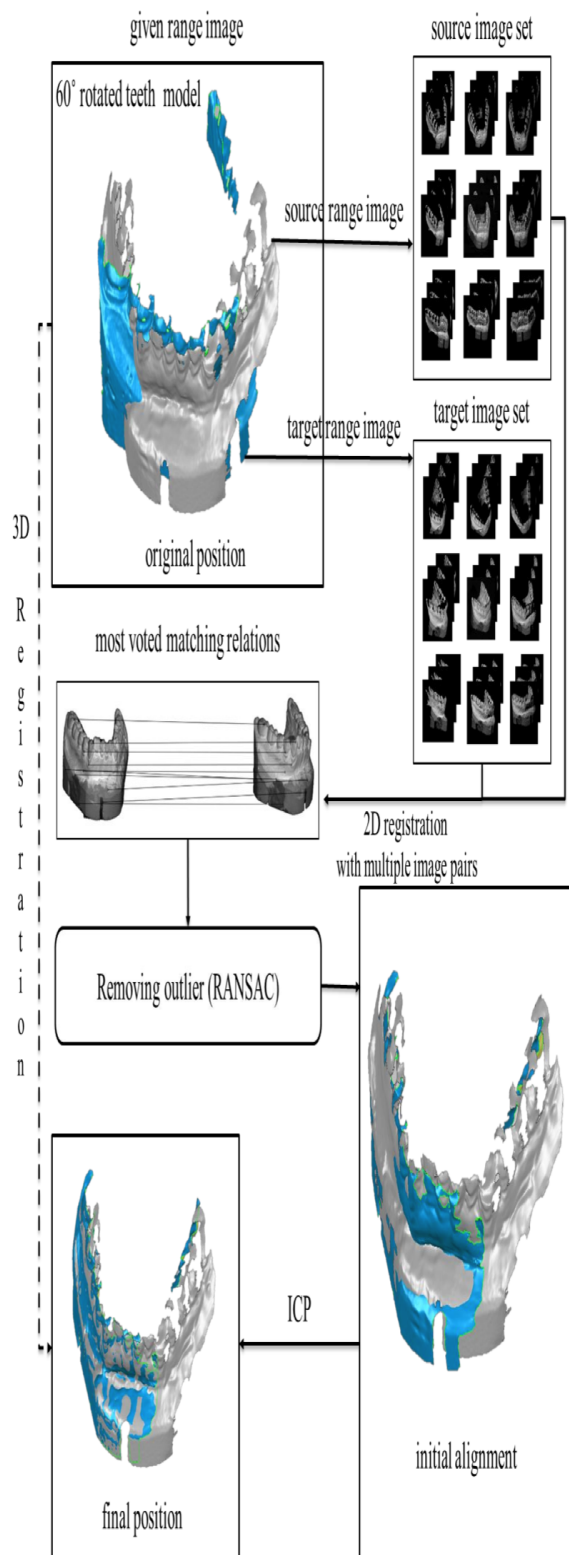
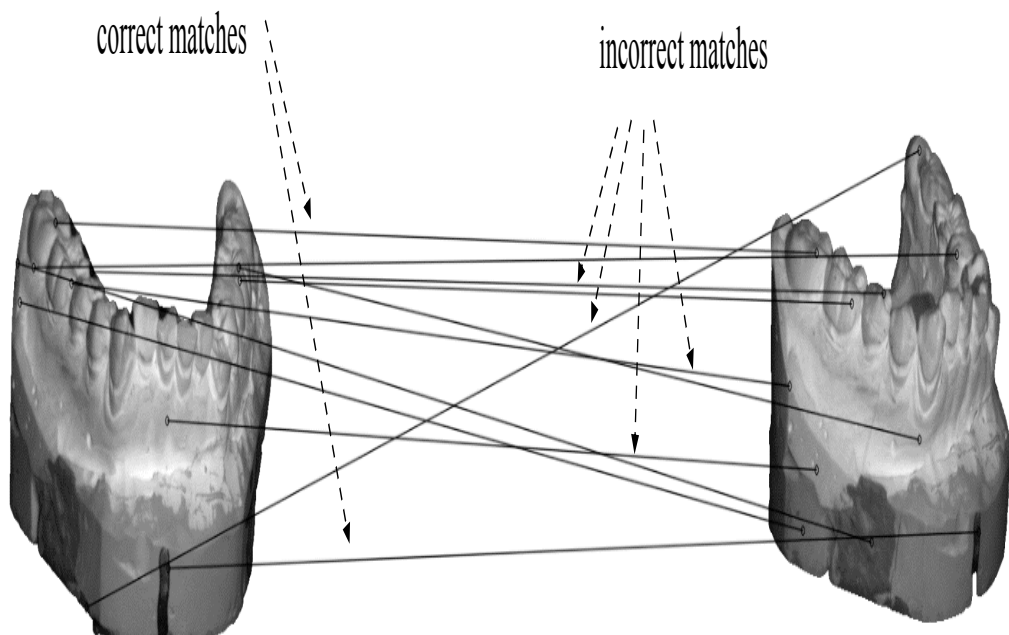


Figure 3. The approach of proposed 3D registration algorithm based on 2D image registration



(a) Interesting points and the feature intensity from a SURF detector



(b) Matching relations from a SURF descriptor

Figure 4. Examples of incorrect SURF matches

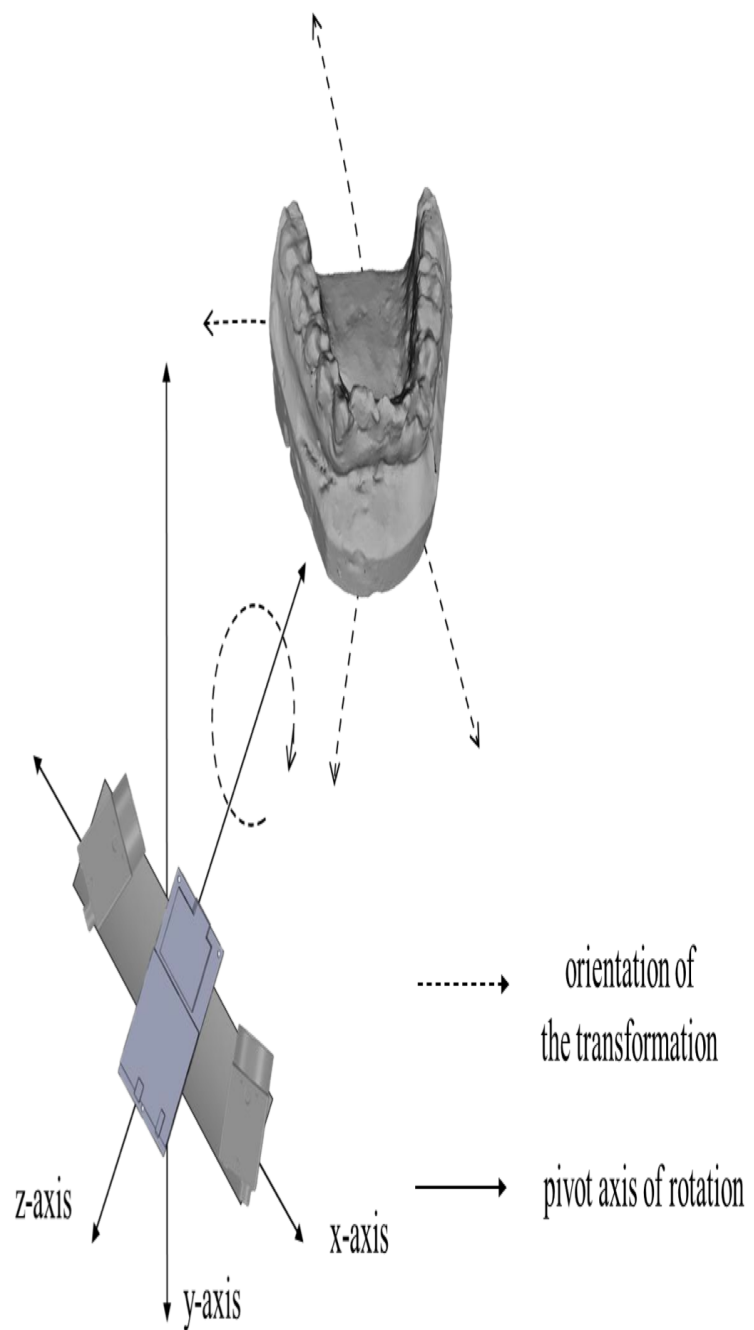


Figure 5. The rotational axes used in transforming the range image

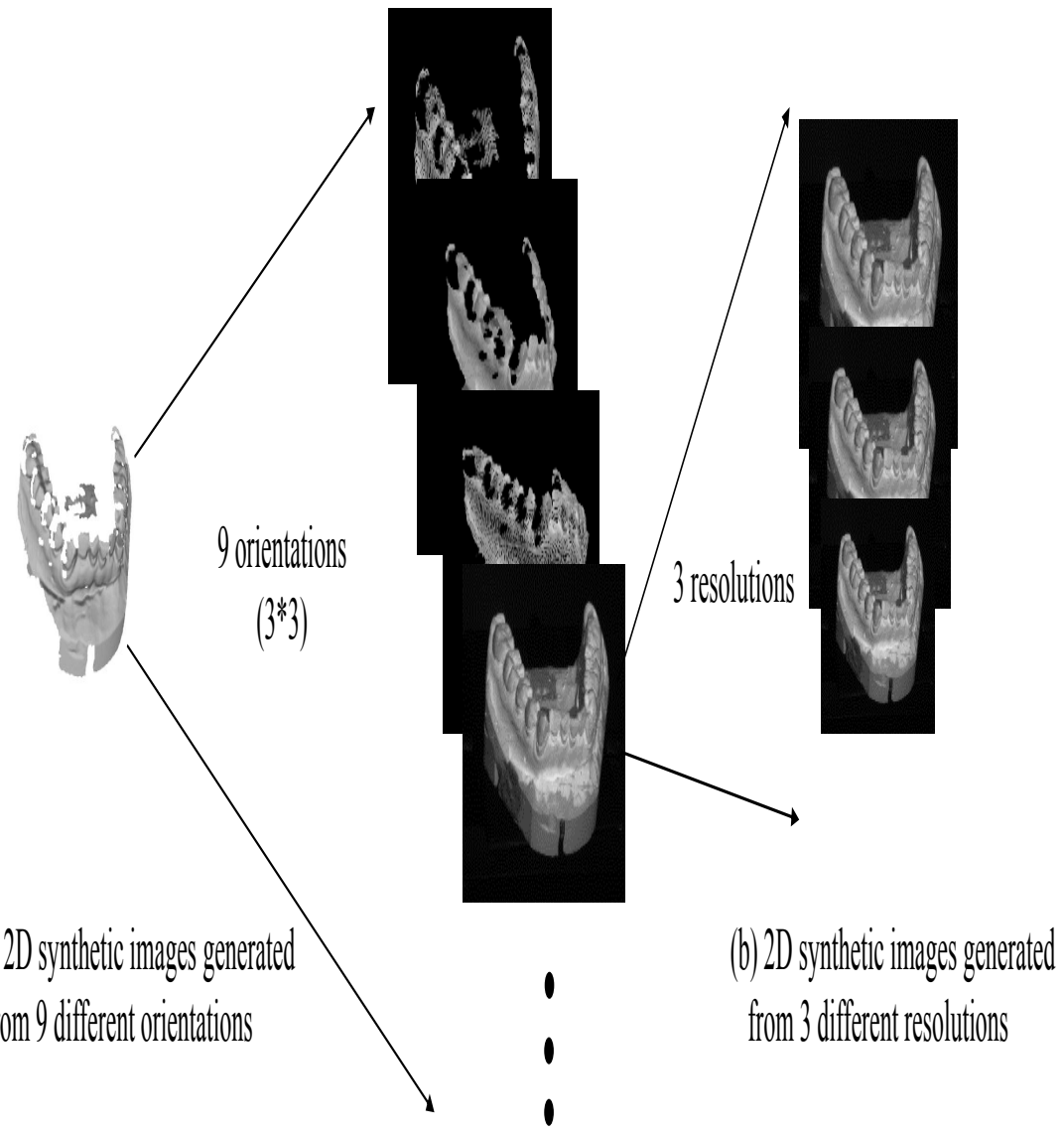


Figure 6. 2D synthetic image set generation from a range image

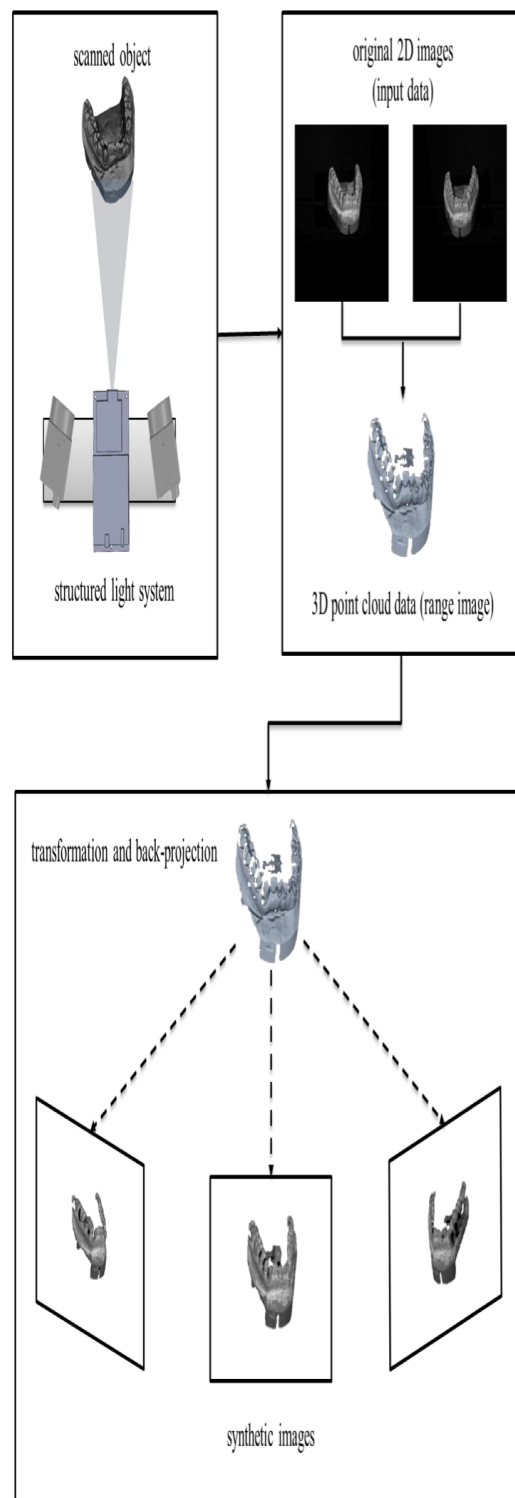


Figure 7. The relationship between the 2D-3D data and the back-projected synthetic images

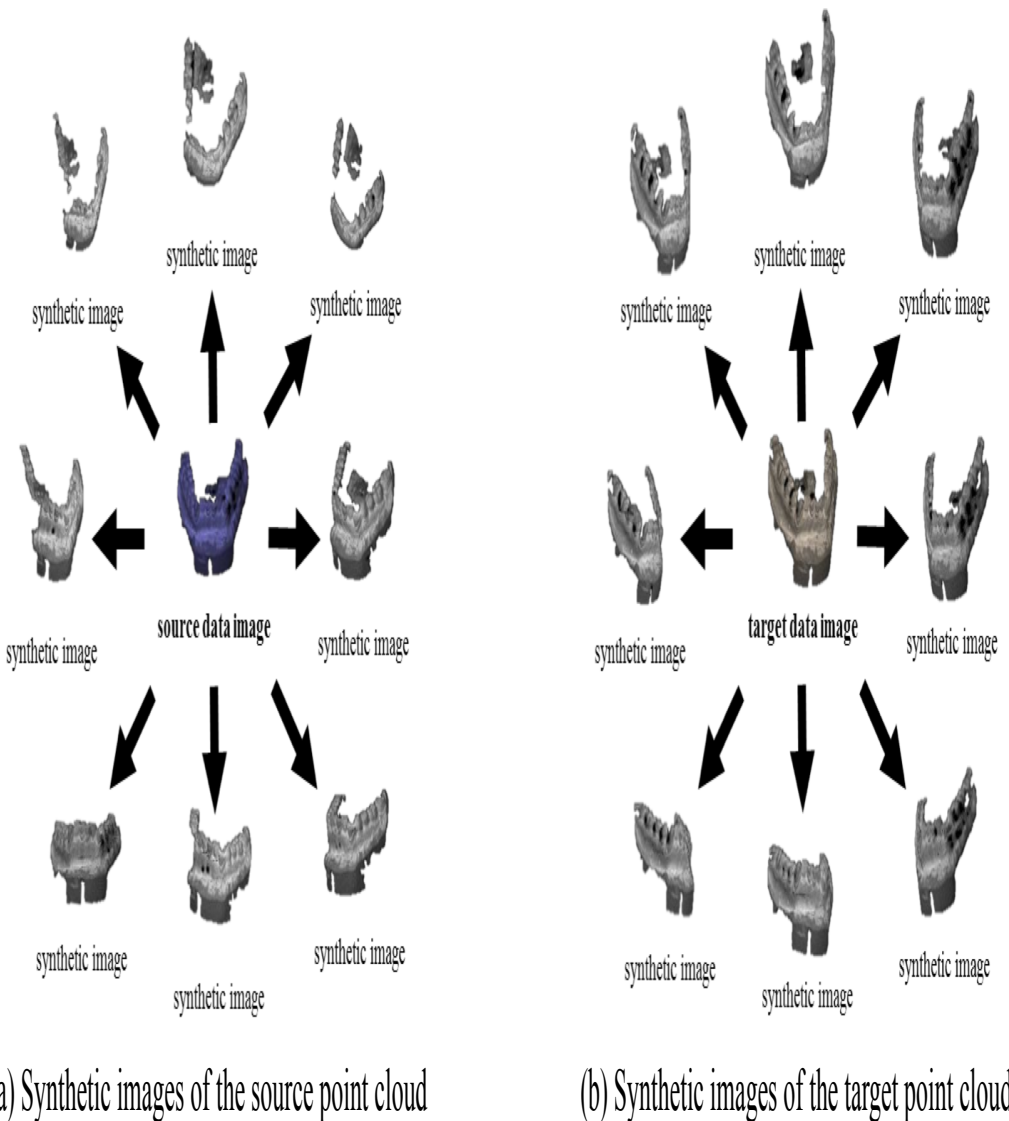
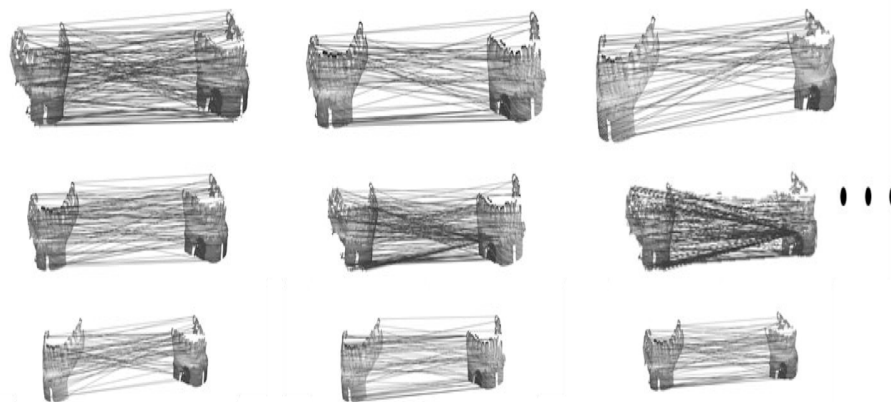
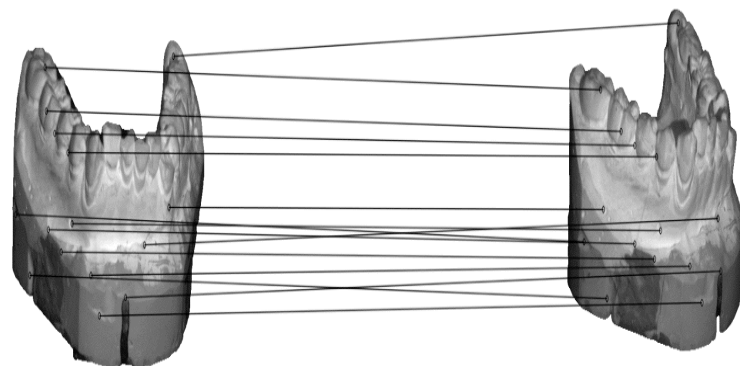


Figure 8. Synthetic image generation from 9 different orientations



(a) Matching relation sets from multiple image pairs



(b) Most voted matching points

Figure 9. Finding matching relations from multiple image pairs

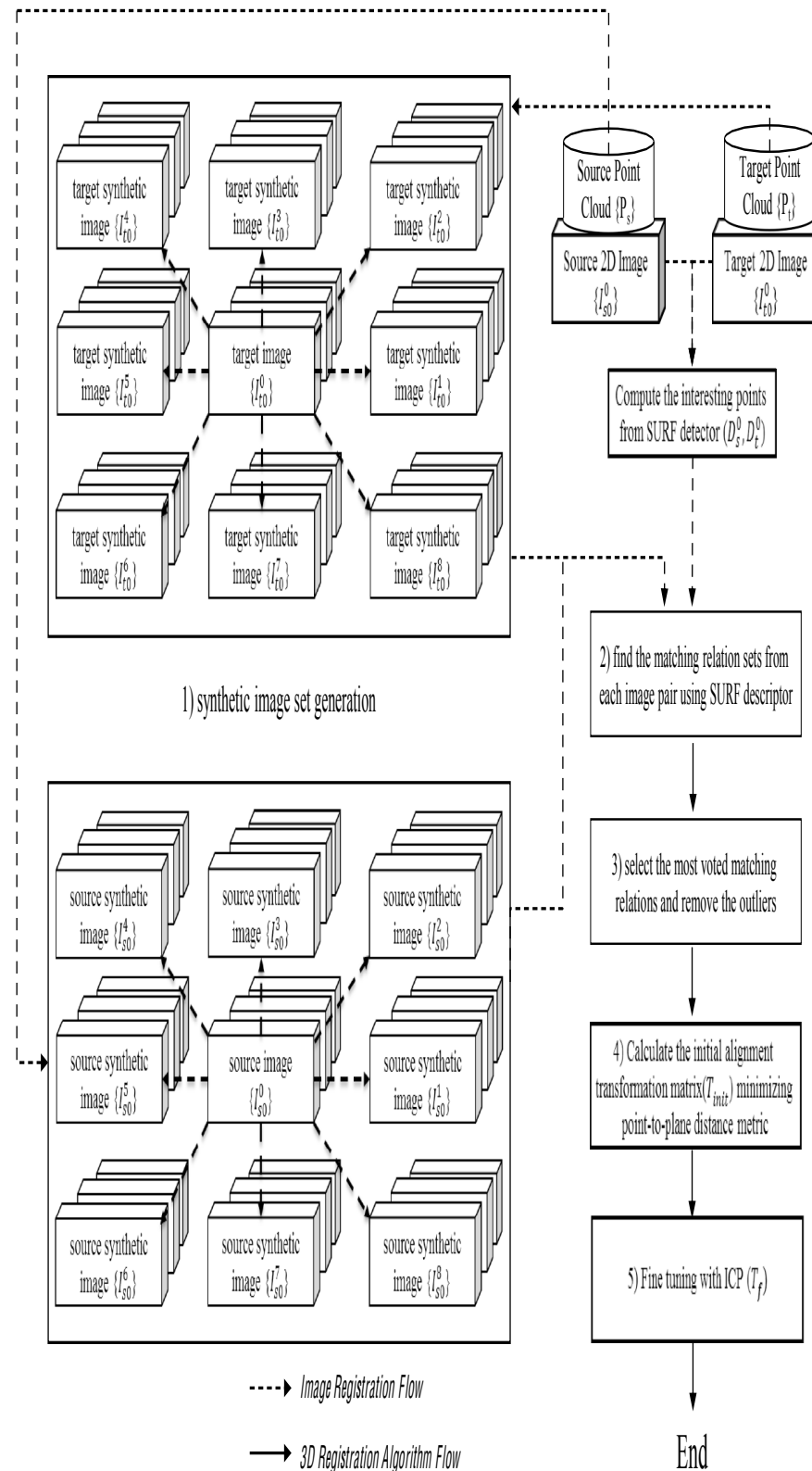


Figure 10. Overview of the proposed registration process

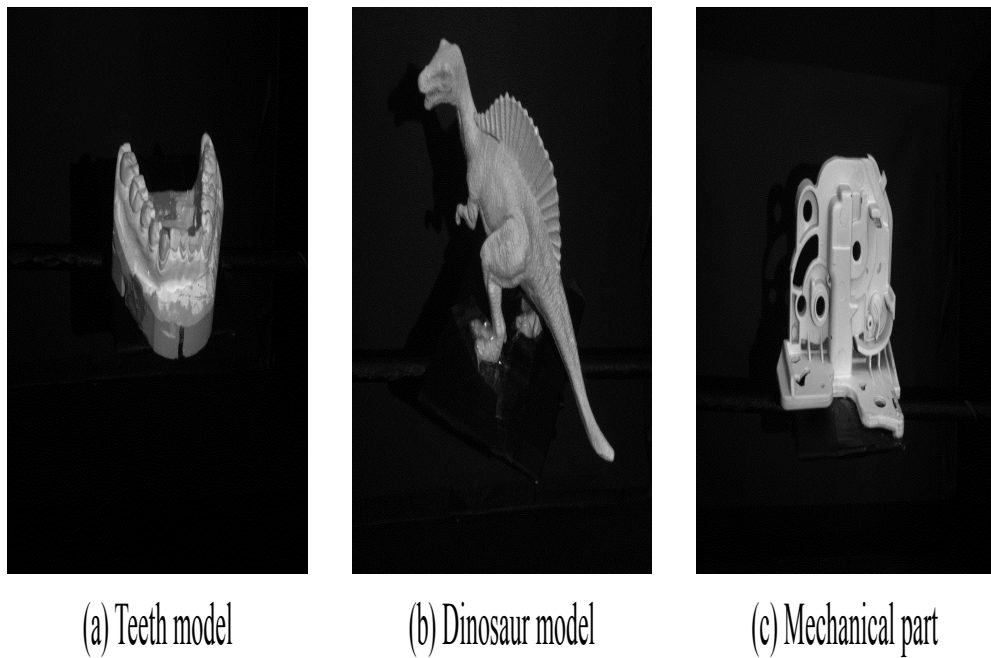


Figure 11. The real-world objects used in the experiments

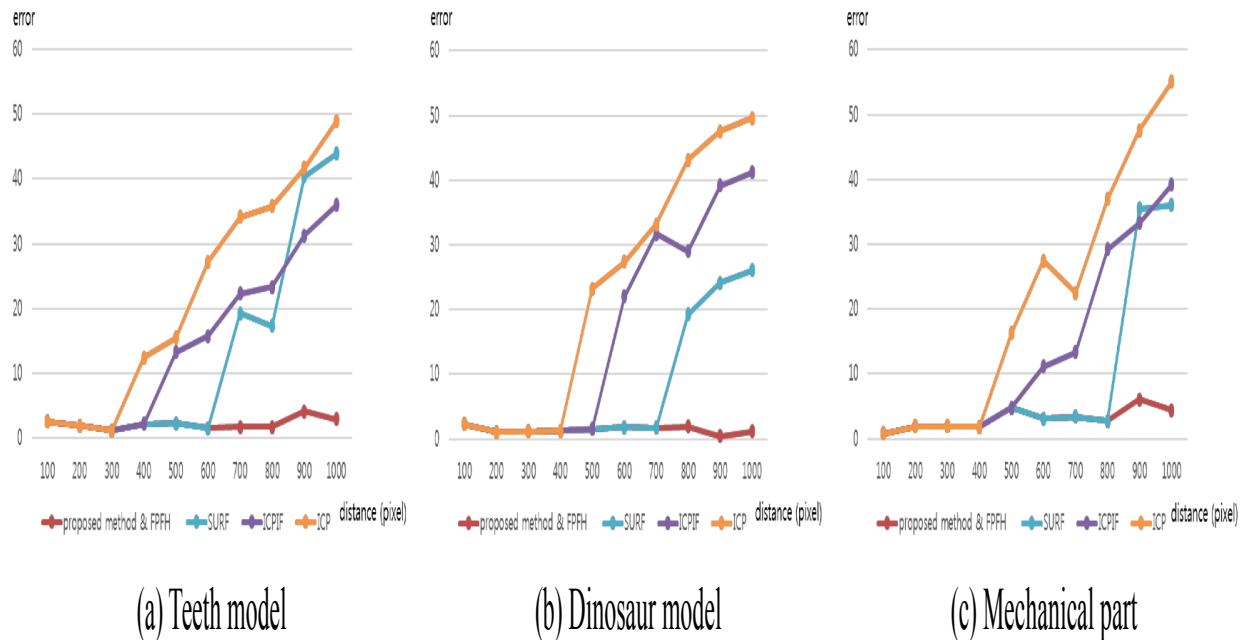


Figure 12. RMSD of the fine registration results using the tested algorithms (translational variation)

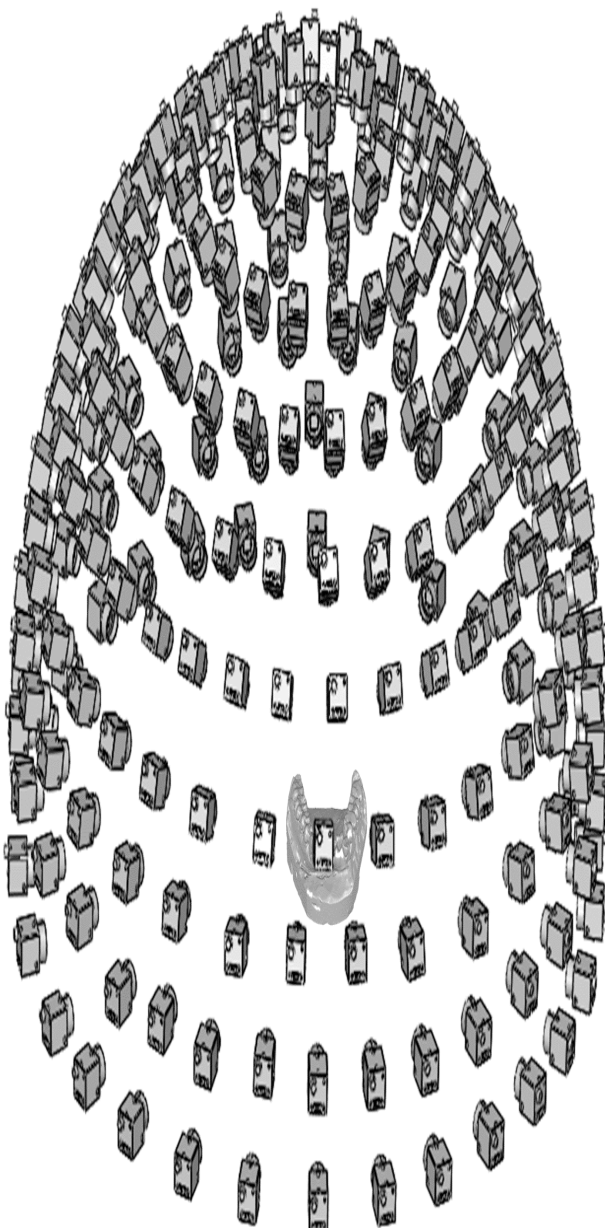


Figure 13. 3D data acquisition on a hemispheric surface

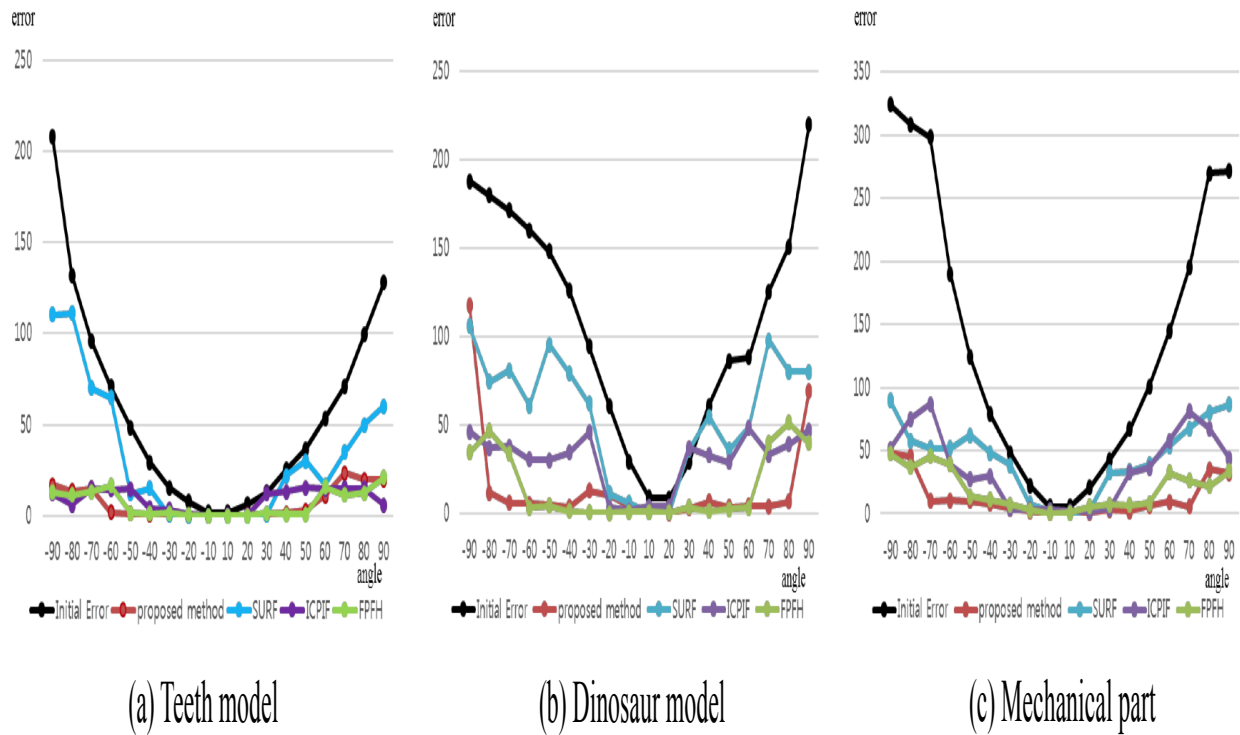


Figure 14. RMSD of the initial alignment results using the tested algorithms (rotational variation)

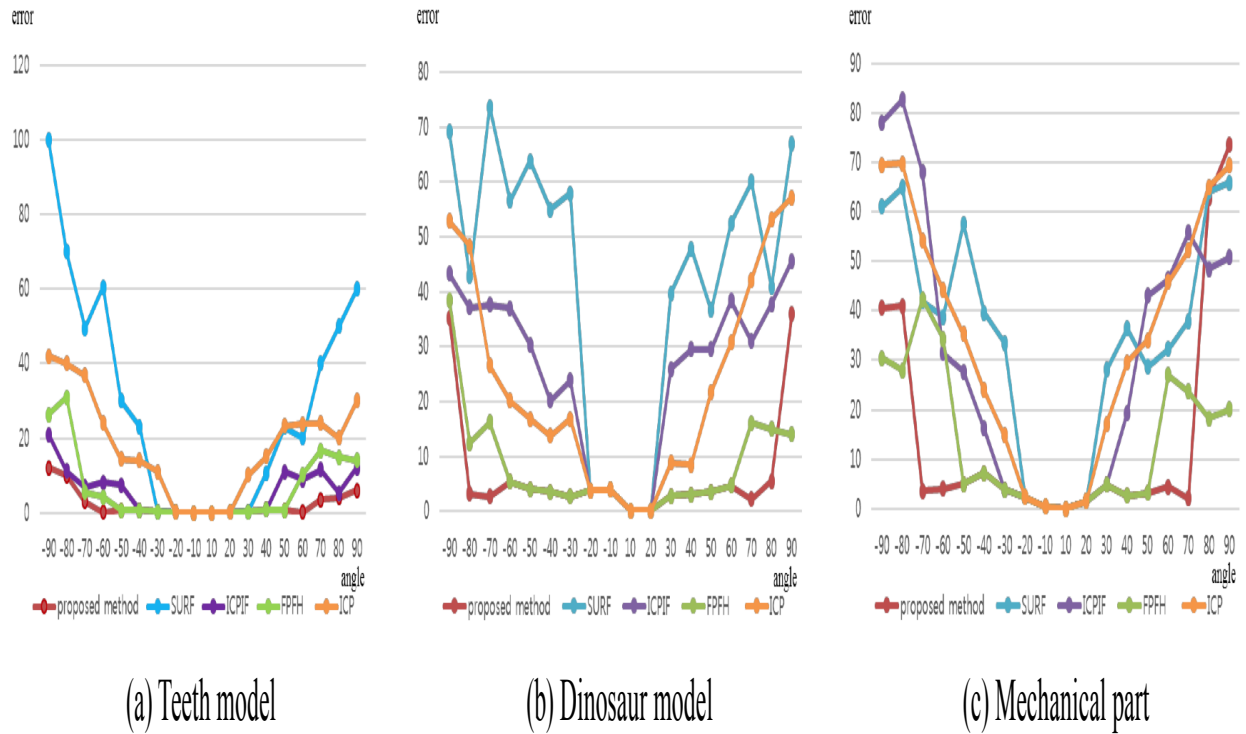


Figure 15. RMSD of the fine registration results using the tested algorithms (rotational variation)

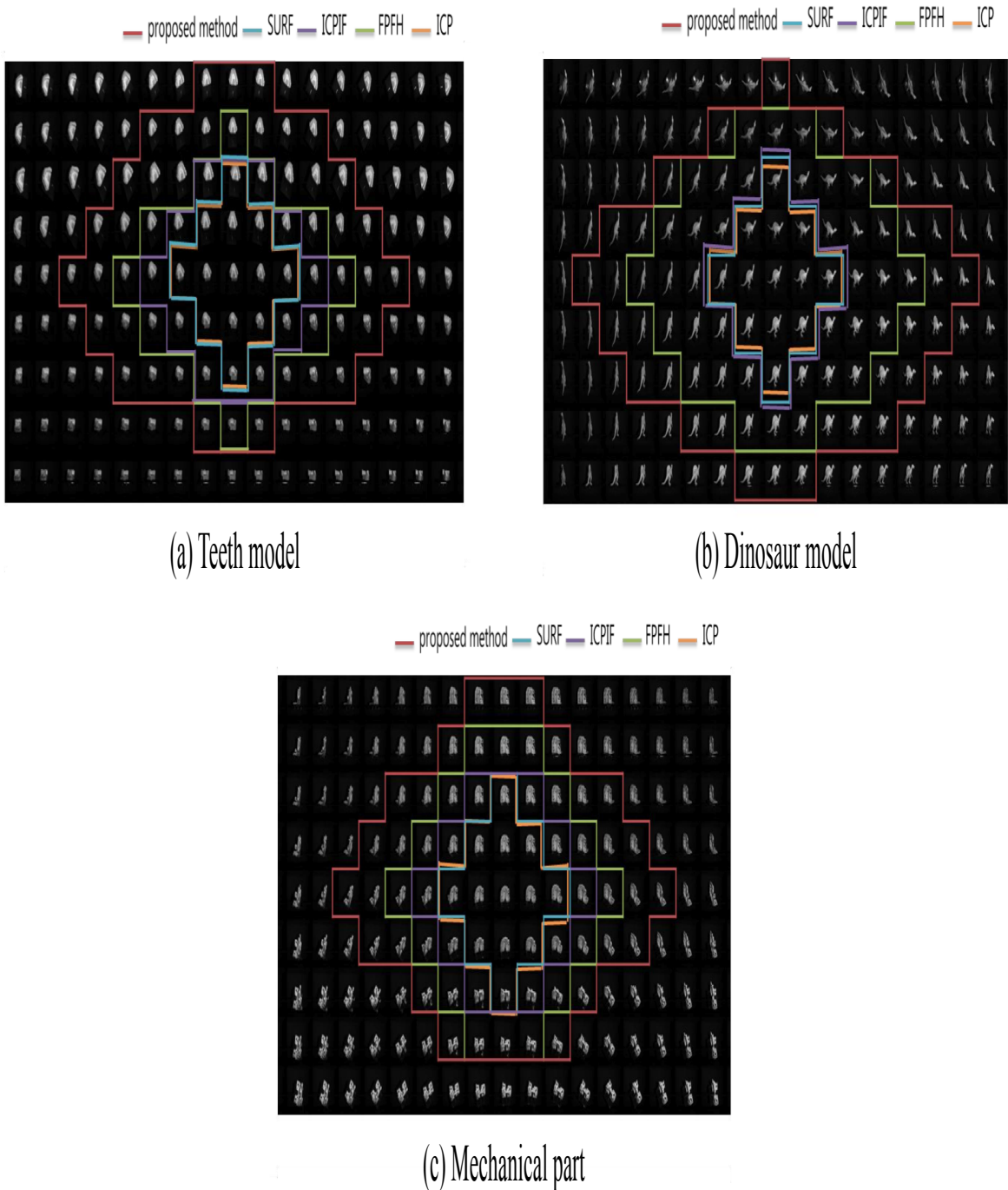


Figure 16. Rotational variation data set images and registration range of the tested algorithms